SPE-170070-MS

Optimization of Coke Resistant Catalyst for Thermal Down-hole Upgrading

Paul Dim, University of Nottingham; Sean Rigby, University of Nottingham; Abarasi Hart, University of Birmingham; Joseph Wood, University of Birmingham

This paper was prepared for presentation at the SPE Heavy Oil Conference-Canada held in Alberta, Canada, 10–12 June 2014.

Abstract

Heavy oil and bitumen are a potential alternative energy source to conventional light crude. However, utilization of these resources can have significant environmental impact. Downhole upgrading offers the potential to improve recovery, and decrease environmental impact. However, use of catalysts to enhance downhole upgrading is limited by the need for a material that can survive the extreme coking conditions arising from the cracking of heavy oil into lighter oil. In this work the potential of hydrogen donors to improve upgrading and enhance catalyst lifetime was considered. In order to extract detailed information on the catalyst structural evolution during reaction a novel integrated adsorption and thermoporometry characterization method was used. This technique allows detailed information to be obtained on the spatial arrangement of pores and their connectivity, as well as size distributions. For catalyst operated at the conditions studied, it has been found that coking arises in smaller pores branching off the larger pores providing access to the catalyst interior. It has been found that use of different hydrogen donors leads to differential survival of open smaller pores in the catalyst, with tetralin providing better protection than cyclohexane or hydrogen gas.

Introduction

Peak production of conventional light oil is likely to occur before 2035 (IEA, 2011). Thereafter there will be a decline in supply if alternative sources are not found and exploited. Heavy oil and bitumen represent a potential alternative to conventional oil. However, heavy oil and bitumen cannot be refined by conventional refineries without upgrading to convert them to synthetic light crude oil (Hart et al., 2013, 2014). Heavy oil and bitumen can be recovered using in-situ combustion. In-situ combustion methods involve burning part of the oil to recover the rest, by using the heat produced from the combustion reactions to reduce the viscosity of the remaining oil and allow it to flow to a producer well. One such method is the Toe-to-Heel Air Injection (THAI) method (Shah et al., 2010). In THAI, air is injected through a vertical injector well to supply the oxidant for a flame front which sweeps through the reservoir. The oil mobilized by the heat from the flame front flows down to a horizontal producer well towards the base of the reservoir. Very high temperatures, up to 600–700 $^{\circ}$C can be obtained in the reservoir. Hence, the oil may undergo pyrolysis, and, also, upgrading reactions due to the natural catalytic activity of the host rock. The CAtalytic upgrading PRocess In-situ (CAPRI) is a way to further enhance the upgrading

arising from the THAI process itself. In CAPRI the horizontal producer well is wrapped around with an annular packed-bed of upgrading catalyst. As the mobilized heavy oil flows towards the producer well it passes through the packed bed of catalyst and undergoes further upgrading reactions. While the catalyst lifetime need only be of the order of a few days, which is the time for the flame front region to pass a particular location, the conditions the catalyst experiences are severe.

The reactions involving heavy oil taking place on the catalyst are highly likely to produce solid carbonaceous deposits, generally called 'coke'. This coke can smother active sites, and/or prevent access of reactants to the catalyst pellets completely by blocking of surface pores. The spatial distribution of coke depends upon the balance between the rates of reaction and mass transfer. The rate of mass transfer is affected by the pore structure of the catalyst pellet. The pore structures of catalysts are generally characterized using techniques, such as gas adsorption or thermoporometry. However, these techniques have problems affecting the accuracy of the pore size distributions for disordered solids that are particularly acute for coked catalysts (Gopinathan et al., 2013). However, these issues, which will be described in more detail below, can be overcome by the novel integrated method described in this paper (Shiko et al., 2012). In this work, rather than using gas sorption or thermoporometry separately, we will combine them into a composite technique. This new technique consists of performing thermoporometry studies using the adsorbate from an adsorption experiment as the probe fluid at different levels of pellet saturation (with adsorbate). As will be seen below, this novel method delivers much more information on the relative proximity of pores affected by coking or left open, and thereby gives a more detailed picture of the coking process. This more detailed picture of pore structure evolution during coking enables a better idea of how to make catalysts more resistant to coking to be obtained.

In this work, we will look at the potential benefits of using a guard bed of activated carbon to protect the catalyst from deactivation, and the impact of the use of various different hydrogen sources for improving upgrading on coking.

Theory

Pore structural characterization by gas sorption is based on the phenomenon of capillary condensation. The Kelvin equation suggests that the logarithm of the relative pressure at which a vapour will condense within a pore is inversely proportional to the pore size. However, the constant of proportionality depends upon the geometry of the pre-existing meniscus before condensation occurs. The relative pressure needed to condense vapour in a through cylindrical pore, with a sleeve-shaped meniscus formed by the surface adsorbed layer, is the square of the relative pressure needed to condense vapour starting from a hemi-spherical meniscus formed at the end of a dead-end cylindrical pore (Rouquerol *et al*., 1999). This sensitivity to meniscus geometry means there is not a monotonic relationship between the applied pressure and the maximum size of pore in which condensation will have occurred for inter-connected, disordered solids. Hence, in a through ink-bottle pore geometry, consisting of a large pore body sandwiched between two narrower necks, the presence of the larger body may be concealed. Condensation in the pore necks via a cylindrical sleeve-shaped meniscus will lead to the development of hemispherical menisci at the entrance to the pore body. If the pressure for this neck-filling process exceeds that for filling of the pore body via a hemispherical meniscus, then the body will also fill simultaneously with the necks, and two pore sizes will appear as one. This 'advanced condensation effect' is a particular problem when studying coking catalysts with gas sorption because a situation of pore-mouth blocking with coke can appear to be more pervasive, complete site-coverage. This is because the entire length of a coked pore may fill with condensate at a lower pressure than before even if just the pore mouth region has been narrowed by coke. It will then look like the size of the whole pore has been reduced by coke deposition, rather than just the entrance.

Thermoporometry makes use of the Gibbs–Thomson effect, whereby small crystals of a liquid located within pores melt at a lower temperature than the bulk liquid. The melting point depression is inversely proportional to the pore size. The melting process for the frozen phase is initiated from existing molten

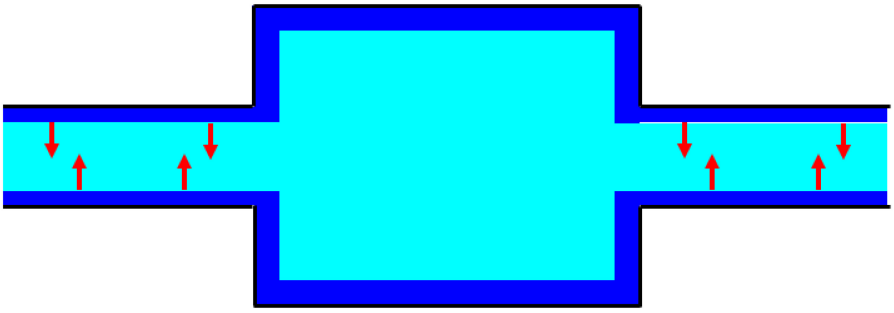

Figure 1—Schematic depiction of the melting process in a cylindrical, through ink-bottle pore system. The dark blue indicates the non-freezing surface liquid-like layer, while the light blue indicates the bulk frozen fluid. The arrows indicate the direction of the meniscus on initiation of melting from sleeve-shaped menisci in the pore necks.

phase, such as the liquid-like layer that is always retained at the pore wall for ice crystals that do not wet the solid. This is shown in Figure 1 for a through ink bottle pore model (position A); the arrows show how the liquid-like layer initiates the melting process and this melting mechanism is said to occur via sleeve-shaped menisci. For such a melting mechanism, the smaller necks will melt first, and, then, as the temperature is raised, the large pore will also melt. Therefore, this type of melting event would give an accurate measurement of the both the neck and body sizes.

However, in cylindrical pores, melting could occur at a lower temperature via a hemispherical meniscus (between solid and molten phases), than it would via a sleeve-shaped meniscus. For the through ink bottle pore in Figure 1, melting is initiated in the outer narrow necks from the thin cylindrical sleeve of permanently unfrozen liquid-like fluid that exists at the pore wall. Once the necks have become fully molten, a hemispherical meniscus will have consequently formed at both ends of the larger pore body. The hemispherical menisci could then initiate the melting process in the large pore provided the larger pore radius is smaller than the critical size for melting via a hemispherical meniscus at the current temperature. In that case the larger pore would melt at the same temperature as the smaller pore. Hence, what is in actuality two different pore sizes, would appear as just one from the melting curve.

While, as has been seen above, both gas sorption and thermoporometry are affected by pore-pore interaction phenomena, leading to a narrowing (relative to reality) of the measured pore size distribution, the critical ratio of the sizes of neighbouring pores when these effects occur is different. Hence, an integrated combination of the two techniques can be used to detect these effects in each other, and infer information on the proximity of pores of given sizes.

Method

CAPRI, the catalytic extension of the THAI process, was investigated using a fixed bed microreactor and laboratory scale experimental rig for heavy crude oil upgrading in the presence of hydrogen donors, such as hydrogen gas, or solvents like cyclohexane and tetralin at two different ratios of THAI oil/Hydrogen donor solvent of 9:1 and 5:1. To simulate the downhole CAPRI process, partially upgraded (THAI feed 3, dentoted T3; 14 ^{o}API and viscosity 1.091 Pa.s) Kerrobert, Canada, heavy crude oil was used as feed under previously optimised operating temperature of 425 °C and 20 barg pressure in a nitrogen atmosphere using HDS/HDT CoMo/Alumina catalyst. The spent catalyst samples for which the pore structure was characterized using the integrated adsorption-thermoporometry method include the fresh and 4 coked Commercial catalyst CoMo/γ-Al2O3 samples, as shown in Table 1.

The methods for the characterization studies of the fresh and spent catalyst samples were as follows. The samples were saturated with water using a Series 3 Climate chamber TAS apparatus at 25°C and Relative Humidity (RH) of 95 or 100% respectively. About 15–30 mg of the partially-, or fully-, saturated samples were sealed into a pre-weighed DSC aluminium hermetic pan (TA Instruments, Part #900793.901

Table 1—Spent catalyst samples studied in this work

Sample code	Sample description
A	CoMo/alumina + H_2 in feed
B	CoMo/alumina + Activated carbon guard bed + THAI 3 experimental oil and cyclohexane (9:1 ratio)
C	CoMo/alumina + Activated carbon guard bed + TEO
D	CoMo/alumina + Activated carbon guard bed + THAI 3 experimental oil and tetralin (9:1 ratio)

Table 2—Results of reaction studies

Reactants	Coke content (wt.%)	Average API gravity rise (deg.)	Viscosity reduction (%)
CoMo + AC + Feed oil/Cyclo (9:1) + N_2	28.21	2.8 ± 0.7	87.0
CoMo + AC + Feed oil/Cyclo (5:1) + N_2	26.55	2.6 ± 0.7	86.0
CoMo + AC + Feed oil/Tetr (9:1) + N_2	26.31	3.0 ± 0.8	89.0
CoMo + AC + Feed oil/Tetr (5:1) + N_2	27.74	2.9 ± 0.7	86.7
CoMo + AC + Feed oil + H_2	26.58	3.3 ± 0.9	86.5

Notes: cyclo = cyclohexane, Tetr = Tetralin and THAI 3 = Feed oil, AC = Activated carbon guard bed and $CoMo/Al_2O_3$

for bottom and Part #900794.901 for lid). The DSC pans were weighed after addition and sealing of the saturated samples. The pan was subsequently introduced into the furnace of the DSC.

A differential scanning calorimeter (Q10 DSC, TA Instruments) equipped with a cooling unit (RCS, Refrigerated Cooling System) for controlled cooling and sub-ambient temperature operation was used. A constant furnace atmosphere was maintained with an in-house nitrogen purge.

The DSC measurements, was performed as follows, the sample was cooled to −50 °C and that temperature was maintained for 30 min to ensure that all of the water was frozen. After that, the sample was heated to 5 °C at a heating rate of 0.5 °C/min and the temperature was maintained for 10min. After completing the DSC measurements, the sample pans were reweighed to check if water had escaped during the experiment. The DSC measurements were carried out repeatedly on three specimen of each sample, over the same conditions. It is important to use the same heating rate throughout experimental run; otherwise the results are influenced by the heating rate. This procedure was repeated using two further heating rates of 1.0 and 1.5°C/min, respectively, to check whether findings were independent of heating rate. No significant effect of heating rate was observed, and thus the data reported is for 1.5°C/min. The data were analysed assuming a Gibbs-Thomson parameter of 50 K nm^{-1} (based on diameter), typical for oxide materials.

Results

The results from the reactor studies are summaried in Table 2.

The nitrogen sorption isotherms for fresh catalyst have been reported previously (Hart et al., 2014). Figure 2 shows the DSC curves for the water in fresh catalyst equilibrated at different relative humidities. At 75% RH the size distribution is very broad, with the modal peak at ~2.5 nm and a pronounced shoulder at ~4 nm. As the RH is increased to 85% and more water is adsorbed, then the DSC modal peak shifts to a larger size of ~5 nm, but remains relatively narrow. As the RH is increased further to 95%, the modal peak becomes substantially broadened towards larger pore sizes. In the final dataset where the RH has been increased to 100%, the modal peak of the DSC curve shifted to lower size of ~3.5 nm. The shift in the modal peak position suggests that, as RH is increased from 75% to 95% steadily larger pore sizes are filled with water. Once the final empty pores are filled by increasing the RH to 100%, the change in the direction of the movement of the modal peak shift with increased RH signified the onset of substantial percolation of the melting front due to the pervasiveness of advanced melting. Pores of size ~3.5 nm are facilitating the advanced melting of a large fraction of larger pores, and thus must be in immediate

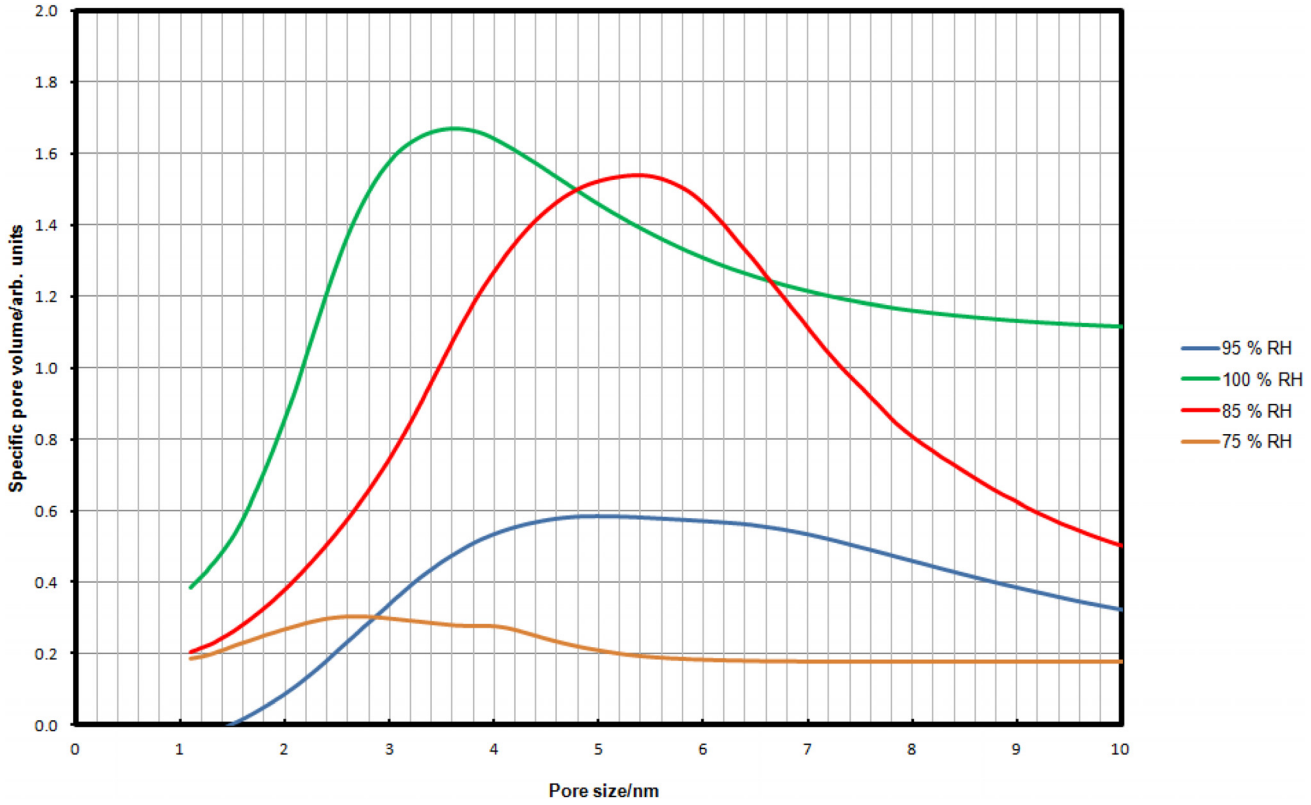

Figure 2—DSC thermoporometry melting curve pore size distributions (histograms) for fresh CoMo catalyst for water saturation equilibrated at four different relative humidities.

proximity these pores. When the potential for significant advanced melting exists (as the highest RH results suggest occurs for the CoMo/alumina catalyst studied here), when the melting curve peak broadens, as it does at intermediate RH values, this suggests the water is adsorbing at these RH values is doing so in relatively segregated regions of the pellet, as no advanced melting occurs to obscure the presence of larger pores.

Figure 3 shows the DSC curves for fully saturated samples of fresh catalyst and the various catalysts discharged following upgrading reactions under different conditions. It can be seen that the general finding is that the modal peak of all of the used catalyst samples has shifted from ~3.5 nm for the fresh catalyst to ~5–6 nm. However the width of the DSC curve peak declines in the order C to D to B to A. Since coking does not lead to the creation of larger pores, but, rather, the opposite. This suggests that the coking has reduced the incidence of advanced melting present in the fresh catalyst. This could occur if the smaller pores facilitating melting for the larger pores were either blocked entirely, or reduced in size such that they fall below the critical size to permit advanced melting. The differences in the apparent width of the size distribution for different spent catalysts suggest that more smaller pores are preserved under some conditions than others. More smaller pores are increasingly preserved in the order A, B, D, to C. However, the similarity in the position of the modal peak for all spent catalysts suggests that the particular small pores (that facilitate advanced melting at low temperature) in close proximity to the larger pores are lost in all conditions.

Figure 4 shows the DSC curves for fresh and spent catalyst samples after partial saturation with water equilibrated at 95% RH. It can be seen that the position of the modal peak is similar for all samples, including the fresh catalyst. This contrasts with the corresponding data obtained at 100% RH, where the modal peak for the spent catalyst samples was significantly displaced relative to that of the fresh catalyst. The position of the modal peak for the spent catalysts has declined very slightly from around 5–6 nm to

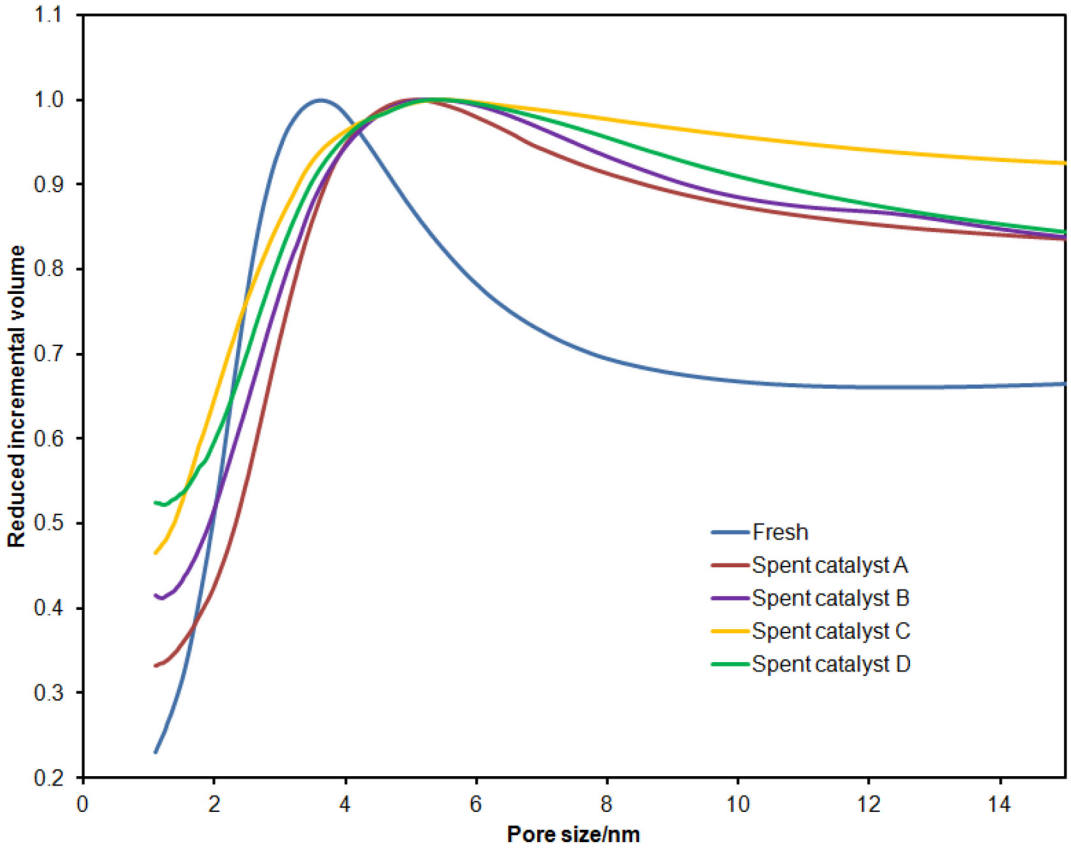

Figure 3—Pore size distribution obtained from DSC thermoporometry melting curve for fully saturated fresh and spent CoMo catalyst samples. The curve represents a histogram of pore size against incremental volume (reduced by maximum incremental volume).

around 4–5 nm. The modal peak for the fresh catalyst is at about 5 nm, and is the narrowest of the samples studied. The similarity of the position of the modal peak for fresh catalyst equilibrated with water vapour at 95% RH to the position of the modal peaks for spent catalysts at both 95% and 100% RH suggests that those pores lost to coking are likely to be the same pores in the fresh sample that facilitate advanaced melting of the pores that fill with condensed water at the highest vapour pressures corresponding to RH between 95% and 100%.

The overall pattern of the findings given above can be understood in terms of a simple corrugated pore model. The model consists of a series of cylindrical pore elements of different diameters arrayed in series. The entrance to the pore from outside the pellet enters a medium sized pore segment, followed by large and small segments in that order. During adsorption of water vapour, if the ratio of sizes of neighbouring pores exceeds the critical value for advanced adsorption, then the three different pores will fill independently. However, if the ratios of the sizes of the large and medium pores to the small one does not exceed the critical ratio for advanced melting, then the modal melting peak will first shift from low to higher temperature as the, initially segregated, small and medium segments fill up, but then shift back to low temperature when the intermediate large pore fills, since then a pervasive pathway would allow the melting front is to advance from the small pore throughout the pore system at a lower temperature. If the interior small pore segment is completely blocked by coking in the spent catalyst, then the medium and large pore segments would still remain accessible to the outside and condensing vapour. Hence, the modal melting peak for a fully water-saturated pore space will correspond to the size of the medium-sized pore segment, as melting would be then initiated at the medium pore segment, with advanced melting of ice within the large segment. At the water saturation level equilibrated with 95% RH, the large pore segment

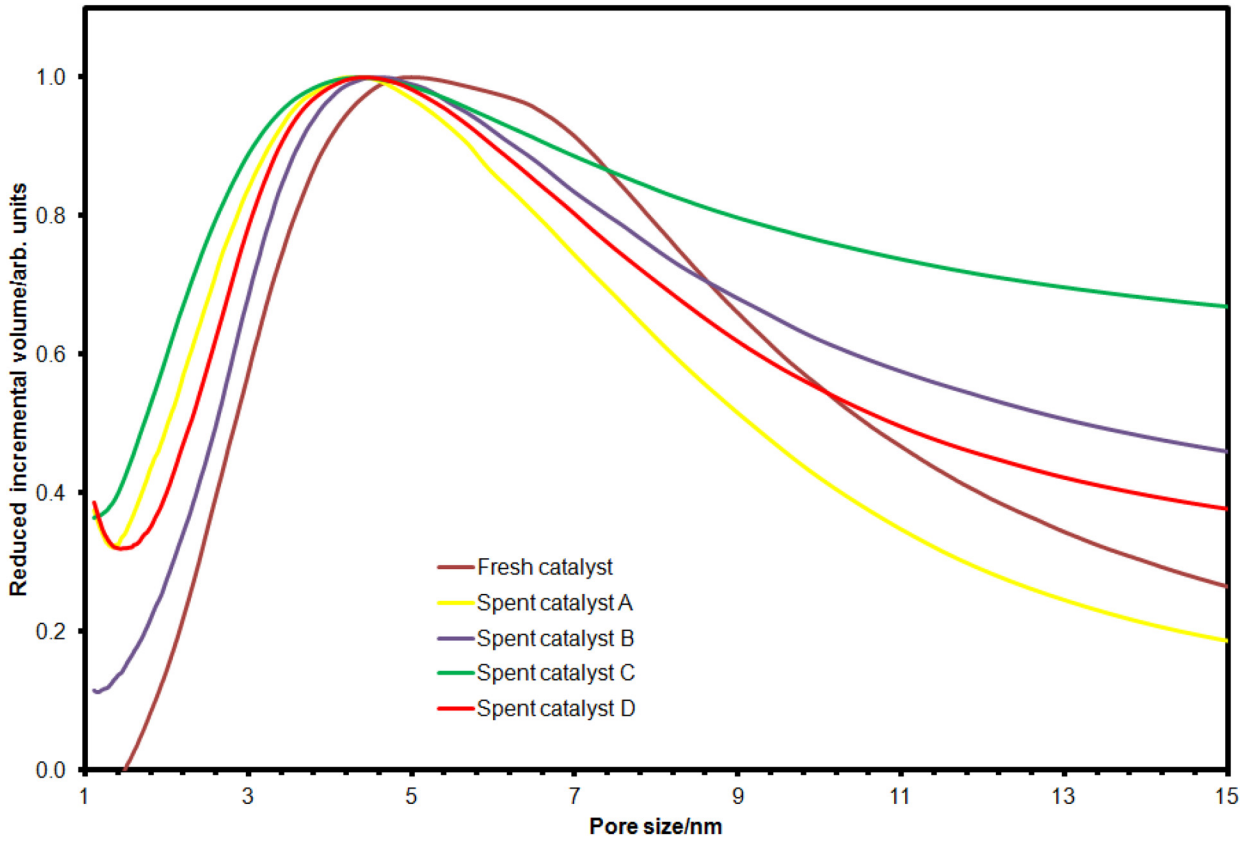

Figure 4—Pore size distribution obtained from DSC thermoporometry melting curve for partially saturated fresh and spent CoMo catalyst samples equilibrated at 95% RH. The curve represents a histogram of pore size against incremental volume (reduced by maximum incremental volume).

would not be filled, and the melting modal peak will be dominated by the medium pore segment size for fresh and coked catalysts, as adavanced melting cannot arise in either case.

Conclusions

For the reaction consitions studied here the coking reactions lead to the blockage and loss of internal smaller pores. The similarity of the positions of the modal peaks for the DSC melting curves for the fully-saturated discharged catalysts suggests that the degree of advanced melting is similar in each sample, and thus the effects of the coke on over connectivity are similar in each case. However, the differences in the widths of the modal peak in the melting curves for the spent catalysts suggests that some reaction conditions (use of TEO and tetralin) preserve the smaller pores in the catalyst better than others. In particular the presence of activated carbon guard bed leads to better preservation of the smaller pores.

References

Gopinathan, N., Greaves, M., Wood, J., Rigby, S.P. (2013). Investigation of the problems with using gas adsorption to probe catalyst pore structure evolution during coking. *Journal of Colloid and Interface Science* **393,** 234–240.

Hart, A., Shah, A., Leeke, G., Greaves, M., Wood, J. (2013). Optimization of the CAPRI process for heavy oil upgrading: Effect of hydrogen and guard bed. *Industrial and Engineering Chemistry Research* **52**: 15394–15406.

Hart, A., Leeke, G., Greaves, M., Wood, J. (2014). Downhole heavy crude upgrading by CAPRI: Effect of hydrogen and methane gases upon upgrading and coke formation. *Fuel* **119**: 226–235.

International Energy Agency (IEA) (2011). *World Energy Outlook*. ISBN 978 9264 12413.

Rouquerol, F. Rouquerol, J. Sing, K. (1999). *Adsorption by Powders and Porous Solids: Principles, Methodology and Applications*. Academic Press, London.

Shah, A., Fishwick, R.P., Wood, J., Leeke, G., Rigby, S.P., Greaves, M. (2010). A review of novel techniques for heavy oil and bitumen extraction and upgrading. *Energy and Environmental Science* **3**: 700–714.

Shiko, E., Edler, K.J., Lowe, J.P., Rigby, S.P. (2012). Probing the impact of advanced melting and advanced adsorption phenomena on the accuracy of pore size distributions from cryoporometry and adsorption using NMR relaxometry and diffusometry. *Journal of Colloid and Interface Science* **385,** 183–192.